FORMATION OF PLANETESIMALS IN THE SOLAR NEBULA

S. J. WEIDENSCHILLING
Planetary Science Institute

and

JEFFREY N. CUZZI
NASA Ames Research Center

This chapter describes the evolution of solid particles in the solar nebula (or other circumstellar disk). Motions of bodies $\lesssim$km in size were dominated by gas drag rather than gravity. An original population of microscopic grains had to produce > km-sized planetesimals before gravitational accretion of planets could begin. Planetesimals probably formed by coagulation of grain aggregates that collided due to differential settling, turbulence, and drag-induced orbital decay. Growth of such aggregates depended on sticking mechanisms and their mechanical properties, which are poorly understood. Their growth was aided by concentration of larger bodies toward the central plane of the disk. The nebula could remain optically thick during this process. It is unlikely that a particle layer formed by settling would undergo gravitational instability, as a small amount of turbulence (e.g., $\alpha \sim 10^{-4}$ in a convective disk) would keep the particle layer from reaching the critical density. This conclusion is independent of the particle size, as even large bodies do not effectively decouple from the gas. Even in a laminar disk, shear in the particle layer would generate enough turbulence to keep it stirred up. This shear-induced turbulence produces complex flow patterns that could result in radial transport and size sorting of particles.

I. INTRODUCTION

The most widely accepted theory of the origin of planets is that they formed by accretion from an initial population of small solid bodies, or planetesimals, in orbit about the Sun. When their orbits intersected, collisions and binding by self-gravity resulted in growth of larger bodies, which eventually reached planetary size. The usual assumption, used as the starting a point for most calculations of planetary accretion (cf. Chapter by Lissauer and Stewart), is that planetesimals had initial sizes in the range 1 to 10 km. This is large enough so that they moved in Keplerian orbits, relatively unaffected by forces other than gravity. In a dynamical sense, there was little difference between a km-sized planetesimal and a planet some 10^4 times larger. In contrast, smaller bodies were dominated by their interactions with nebular gas, while it was present. Planetesimals must have formed from smaller bodies, i.e., surviving

presolar grains and/or condensates from the gas of the solar nebula. With presently available observational techniques, dust is the dominant, perhaps only, detectable solid matter in protostellar disks and surrounding newly formed stars (see Chapter by Strom et al.). The dust is the principal source of opacity in optically thick disks. The presence of larger bodies, either planetesimals or planets, must be inferred indirectly. We cannot tell whether dust means that large bodies have not yet formed, or that they are merely hidden within a dusty cocoon.

At one time, it was generally accepted that planetesimals formed by gravitational instability. In that model, dust grains settled to the central plane of the gaseous disk, forming a layer of enhanced concentration. This dust layer became thinner until its density reached a critical value about equal to the Roche density:

$$\rho_c \simeq 3M_\odot/2\pi r^3 \tag{1}$$

where $M_\odot$ is the solar mass, and r the distance from the Sun. At this density, the layer would become unstable to perturbations by its own self-gravity, and develop condensations with a characteristic size

$$\lambda_c \simeq 4\pi G\sigma_s/\Omega^2 \tag{2}$$

where G is the gravitational constant, σ_s the surface density of the dust layer, and $\Omega = (GM_\odot/r^3)^{\frac{1}{2}}$ the Kepler frequency. The mass of a condensation would be $\sim\sigma_s\lambda_c^2$; plausible values of σ_s imply that the resulting planetesimals would have sizes $\sim$1 to 10 km. The quantitative aspects of this model were developed independently by Safronov (1972) and Goldreich and Ward (1973).

The simplicity of this model is appealing, but there are problems that render it untenable, at least in the extreme form of direct conversion of μm-sized dust grains to km-sized bodies by gravity alone, without any other sticking mechanism. Wetherill (1980*a*) warned that ". . . it would be a mistake to conclude that the solar system *must* have developed dust-layer instabilities simply because this does not require specification of sticking processes that are poorly understood, but that quite possibly may have occurred anyway." Weidenschilling (1988) pointed out that gravitational instability depends on quiescent nebula. An extremely small amount of turbulence in the gas would prevent the dust layer from reaching the critical density; in order to do so, its thickness must be $\lesssim 10^{-6}r$. This condition implies turbulent velocities $\lesssim$ one particle diameter s^{-1}, which are implausible for dust grains and unlikely even for macroscopic bodies. Over the last two decades both theory and observations have led away from the simple picture of the solar nebulas a passive reservoir of raw material for making planets. Rather, it was a dynamic, evolving, and sometimes violent place. Small solid bodies were more strongly affected by drag of nebular gas than by gravitational forces, and gas was probably turbulent. Formation of planetesimals must have involved some collisional sticking, at least to form bodies large enough to settle toward

the central plane and begin to decouple from the gas. In the follow sections we describe briefly some of the effects of particle/gas interaction in the solar nebula (for a fuller account, see Adachi et al. [1976], Weidenschilling [1977*a*,1980,1984,1988] and Nakagawa et al. [1981,1986]).

II. STRUCTURE OF THE NEBULAR DISK

A zero-order description of the solar nebula is a flattened disk of gas in orbit about the proto-Sun. The process of formation of planetesimals was dominated by the first-order corrections to this picture, i.e., the disk had a finite thickness; its mean rotation was not strictly Keplerian, and may have had turbulent motions; and most importantly, some small fraction of its mass consisted of solid matter. Present observational methods do not constrain the structures of protostellar disks at this level of detail; of necessity, the "solar nebula" described here is essentially schematic.

For simplicity we assume that the surface density Σ has a power law distribution:

$$\Sigma(r) = \Sigma_o(r/r_o)^{-n} \tag{3}$$

where Σ_o is the value at some arbitrary radius r_o. The masses and orbital radii of the planets are roughly consistent with $n = 3/2$ (Weidenschilling 1977*b*). We assume the disk's structure is in equilibrium between gravitational, centrifugal, and pressure forces. If Σ is low enough (disk mass ≤ 0.1 $M_\odot$), the disk's gravity can be neglected, and the force normal to the plane of the disk is simply the vertical component of solar gravity:

$$g_z = \frac{GM_\odot}{r^2}\left[\frac{z}{r}\right] = \Omega^2 z \tag{4}$$

where z is the distance from the midplane. If the local temperature T is independent of z, then the gas pressure at the midplane is (Safronov 1972)

$$P_c = \Omega\Sigma c/4 \tag{5}$$

where c is the mean thermal velocity of the gas molecules (nearly equal to sound velocity), and at other values of z is

$$P(z) = P_c \exp(-z^2/H^2) \tag{6}$$

where $H = \sqrt{\pi}c/2\Omega$ is the characteristic half-thickness of the disk. Other plausible temperature profiles, e.g., adiabatic gradient in the z direction, yield similar values. Typical model disks have $H \leq 0.1r$.

Equation (5) implies a radial pressure gradient. Most disk models have both Σ and T (hence c) decreasing with r, while $\Omega \propto r^{-3/2}$. If we assume that $T(r) = T_o(r/r_o)^{-k}$, then

$$P_c(r) \propto r^{-(n+k/2+3/2)} \tag{7}$$

and $\partial P/\partial r<0$, unless Σ actually increases with r more rapidly than $r^{(3+k)/2}$. The pressure gradient partially supports the gaseous disk against the Sun's gravity; for equilibrium, its rotation must be slightly slower than the Kepler velocity V_k. The fractional deviation is (Weidenschilling 1977*a*)

$$\frac{\Delta V}{V_k} = \frac{-(n+k/2+3/2)}{2} \frac{\Re T/\mu}{(GM_\odot/r)} \tag{8}$$

where $\Re$ is the gas constant and μ the mean molecular weight. Thus, $\Delta V/V_k$ is of order $c^2/{V_k}^2$, or the ratio of the thermal energy of a gas molecule to its orbital kinetic energy. This quantity is typically only a few times 10^{-3}, but even this small deviation from Keplerian rotation has important consequences for solid bodies within the disk.

A. Turbulence

The solar nebula must have been turbulent during its formation from the collapsing protostar, because of velocity discontinuities as the infalling matter struck the disk (Cassen and Moosman 1981). The infall probably did not stop suddenly, but decayed, not necessarily monotonically, over some interval. Another possible source of turbulence was a massive outflow from the proto-Sun, impinging on the surface of the disk (Elmegreen 1978*b*).

Some researchers (ter Haar 1950; Safronov 1972; Hayashi et al. 1985) have concluded that in the absence of such extrinsic stirring mechanisms any residual turbulence would have decayed quickly. This conclusion was based on the stability of a rotating disk against convection in the radial direction This stability would allow a quiescent period of indefinite length, during which planetesimals, or even planets, could form. However, the concept of a laminar nebula was challenged by Lin and co-workers (Lin and Papaloizou 1980; Lin and Bodenheimer 1982; Ruden and Lin 1986), who developed a self-consistent model for turbulence driven by the differential rotation of the disk. If convection occurs normal to the plane of the disk, eddies cause the effective viscosity to be large. Shear in the viscous, differentially rotating disk causes dissipation of energy, and the resulting heating drives the convection. Lin and Papaloizou showed that the disk is unstable to convection in the z direction if it is optically thick and the opacity increases sufficiently rapidly with temperature; both conditions are met if the opacity is due to small grains suspended in the gas. The ultimate energy source for the turbulence is the disk's potential energy in the solar gravity well (viscous spreading causes a net inward flow of gas).

Published models of turbulent accretion disks generally define the turbulent viscosity $\nu_t = \alpha H c$, where α is a coefficient chosen to make this expression correct (cf. Weidenschilling 1988*a*). This expression is appropriate for turbulence acting on the full vertical scale (H) of the nebular gas. If H is taken to be the length scale of the largest turbulent eddies, then the maximum random velocities of gas in those eddies is of order αc, but this should

be regarded as no more than a crude estimate. Lin's early models suggested $\alpha \simeq 1/3$, with convective velocities a significant fraction of the sound speed. A more elaborate analysis of convective instability modes in a rotating disk led Cabot et al. (1987*a*, *b*) to conclude that likely values of α were in the range 10^{-4} to 10^{-2}, or $\nu_t \sim 10^{13}$ to 10^{15} cm^2 s^{-1}. The corresponding turbulent velocities V_t, are $\lesssim 0.01$ c, or less than a few tens of meters per second in the inner part of the disk, and less in the outer regions.

The size of the largest eddies is set by the dimensions of the disk. The energy in those eddies cascades through a spectrum of smaller eddies, down to a size where they are damped by molecular viscosity. Dimensional arguments (Tennekes and Lumley 1972) imply that the rate of dissipation per unit mass is of order

$$\epsilon \sim V_t^3/L \tag{9}$$

where V_t, and L are the velocity and length scales of the largest eddies. The smallest eddies have the so-called "inner scales" of velocity, length and time given by

$$\begin{aligned} u_i &\sim (\nu\epsilon)^{\frac{1}{4}} \\ \ell_i &\sim (\nu^3/\epsilon)^{\frac{1}{4}} \\ t_i &\sim (\nu/\epsilon)^{\frac{1}{2}} \end{aligned} \tag{10}$$

where ν is the molecular viscosity. On smaller scales, the flow is locally laminar, though varying with time. For example, if $V_t = 10$ m s^{-1} and $L = H \simeq 0.05$ AU, then u_i, ℓ_i, t_i are respectively a few cm s^{-1}, a few hundred meters, and a few hours.

III. AERODYNAMICS OF SOLID BODIES IN THE NEBULA

The behavior of an individual solid body in the nebular gas (laminar or turbulent) is largely determined by a single parameter, its response time to the force exerted by gas drag:

$$t_e = mV/F_d \tag{11}$$

where m is the particle's mass and V its velocity relative to the gas. The drag force F_d depends on V and two dimensionless parameters, the Reynolds and Knudsen numbers. The Reynolds number Re is the ratio of inertial to viscous forces; for a particle of diameter d, $Re = Vd/\nu$. The Knudsen number Kn is defined as λ/d, where λ is the mean free path of the gas molecules. At the low gas densities in the solar nebula, λ is typically >1 cm, so Kn is large for typical grains and even aggregates of many grains. In this regime, t_e has the simple form

$$t_e = d\rho_s/2\rho c \tag{12}$$

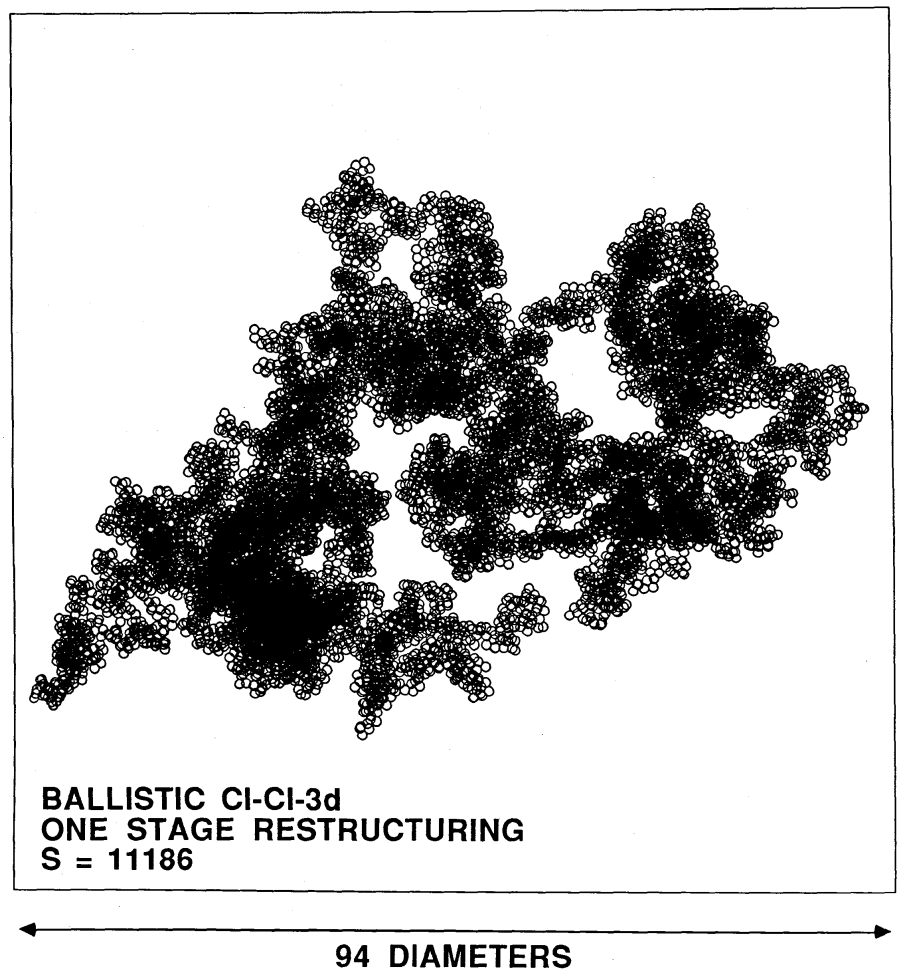

Figure 1. View of a fractal aggregate of dimension $D \simeq 2.1$, generated by a computer model of P. Meakin (cf. Weidenschilling et al. 1989). Fluffy structures resembling this aggregate are found in laboratory studies of particle coagulation (Meakin and Donn 1988), and should have been produced in the solar nebula.

where ρ is the gas density and ρ_s is the particle's density. Expressions for t_e in other in other regimes are given by Weidenschilling (1977*a*).

Equation (12) refers to a spherical particle of diameter d. However, coagulation of solid grains does not produce spherical particles, but rather aggregates with highly irregular shapes (Fig. 1). Such structures have fractal-like properties, i.e., their bulk densities decrease with increasing size (Meakin and Donn 1988), with $\rho_s \propto d^{D-3}$, where D is the fractal dimension of the aggregate. Particle aggregates typically have $D \simeq 2$, so density varies inversely with size. In the regime of large Kn, t_e is proportional to the ratio of particle mass to its projected area. Computer models by P. Meakin (cf. Weidenschilling et al. 1989) give the mass/area ratio for fractal aggregates with $D \simeq 2$ shown in Fig. 2. As one would expect, a low-density aggregate of irregular shape is more strongly coupled to the gas (has smaller t_e) than a dense, compact body with the same mass. The larger cross section also means that the opacity due

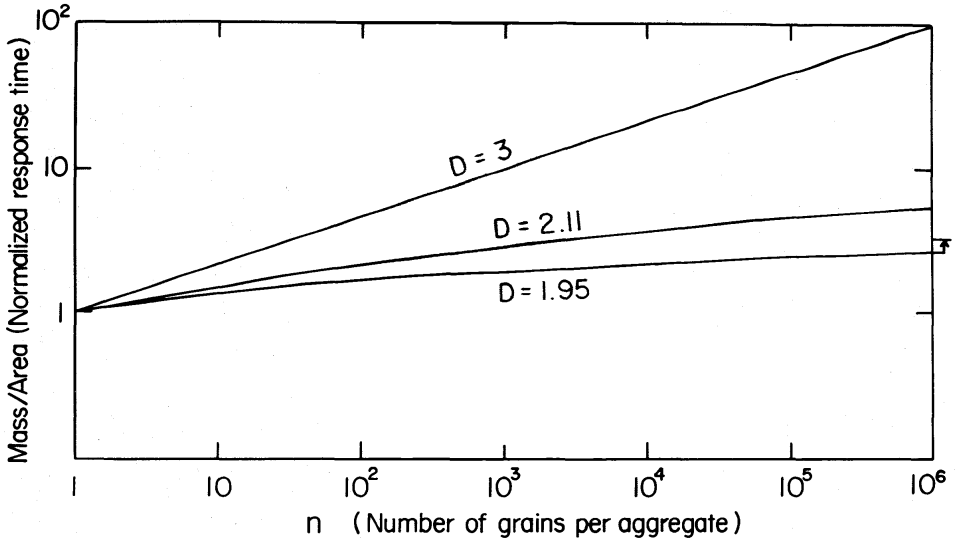

Figure 2. Mass/area ratio (or response time t_e) for aggregates of different fractal dimension D, vs number of grains (or mass). $D = 3$ corresponds to a spherical particle of constant density. Aggregates with $D \simeq 2$ have larger cross sections and smaller t_e, i.e., are more closely coupled to the gas by drag forces than are compact particles of the same mass.

to grains remains relatively high, despite their coagulation.

Solar gravity affects the particle's motion on a time scale of $1/\Omega$, the inverse of the Kepler frequency. If $t_e << 1/\Omega$, drag force dominates and the particle moves with the angular velocity of the gas. A solid body is not supported by the pressure gradient in the gas, and so there is a residual gravitational force in the radial direction. The particle drifts radially inward (relative to the gas) at a terminal velocity

$$V_r = -2\Omega t_e \Delta V. \tag{13}$$

Similarly, the vertical component of solar gravity (Eq. 4) causes a particle at distance z from the central plane to settle vertically at a rate

$$V_z = -\Omega^2 z t_e. \tag{14}$$

A sufficiently large body has $t_e >> 1/\Omega$; its motion is dominated by gravitational forces. Such a body follows a Keplerian orbit, moving faster than the gas. This "headwind" of magnitude ΔV causes the orbit to decay. A circular orbit of semimajor axis a decays at a rate

$$V_r = da/dt = -2\Delta V/(\Omega t_e). \tag{15}$$

The radial velocity has a maximum value of ΔV when $t_e = 1/\Omega$ (Weidenschilling 1977*a*). Bodies of different sizes (or t_e) have relative velocities that are readily found from Eqs. (13–15). Effects of drag on eccentric and inclined Keplerian orbits are discussed by Adachi et al. (1976).

In addition to these systematic motions induced by the nebula's non-Keplerian rotation, particles may have other motions driven by turbulence in the gas. The relevant parameters controlling their behavior are the response time t_e, the inner time scale of the turbulence t_i, and the turnover time of the largest eddies, t_o. If $t_e < t_i$, a particle is effectively coupled to all motions of the gas, down to the smallest eddies. If $t_e > t_o$, it is decoupled from the turbulence at all scales, and can cross the largest eddies. For intermediate values of t_e, the particle responds to eddies larger than some size between the smallest and largest scales. The smallest scales are given by Eqs. (10), while in a rotating system it is generally a good assumption that $t_o \sim 1/\Omega$.

Diffusive transport of particles relative to the mean (nonturbulent) component of gas flow is accomplished mainly by the largest eddies. The viscosity ν_t due to gas turbulence can be expressed as $\overline{v^2} t_o$, where $\overline{v^2}$ is the mean square of the fluctuating part of the gas velocity, and t_o is the mean eddy mixing time. A particle acquires its random velocity v_p by drag interactions with fluid eddies, described by the equation $\dot{v}_p = (v - v_p)/t_e$. Because $\dot{v} \simeq v/t_o$, v_p/v should depend on the time scale ratio t_e/t_o, known as the Stokes number (Crowe et al. 1985,1988). The Schmidt number is defined as $Sc \equiv \overline{v^2}/\overline{v_p^2}$ and, by analogy with the fluid viscosity, a particle diffusion coefficient $D = \nu_t/Sc$ may be written $\overline{v_p^2}$, where $\overline{v_p^2}$ is the mean square fluctuation of the particle velocity (see Appendix below). Safronov (1972) assumed that $t_o \simeq 1/\Omega$, and also argued that a particle would build up a typical velocity $v_p = V_t/(1 + t_e/t_o)$, implying $Sc = (1 + t_e/t_o)^2$. A more careful analysis, including averaging over a size spectrum of rotating eddies, indicates that the Schmidt number becomes simply (Völk et al. 1980)

$$Sc = 1 + t_e/t_o$$

or

$$v_p = V_t/(1 + t_e/t_o)^{\frac{1}{2}}. \tag{16}$$

For small Stokes numbers, Sc is near unity since the particles respond to the eddies almost immediately, like the fluid molecules themselves. The Schmidt number becomes large at high Stokes numbers because of the reduced coupling of the particles to the eddies.

The relative velocity between two particles embedded in turbulent gas is more complex, and depends on t_o, t_i, and the value of t_e for each particle. These relative velocities are needed to study collisions between particles and accretion that may result (Sec. V). A first solution by Völk et al. (1980) neglected the inner cutoff scale of the turbulence spectrum. An improved solution by Mizuno et al. (1988) takes this cutoff into account; its effect is to decrease the relative velocities of small grains for which $t_e < t_i$. Two bodies with the same value of t_e have no systematic relative motion, but will have nonzero relative velocities due to turbulence (small particles may have significant thermal motion as well). Relative velocities as a function of

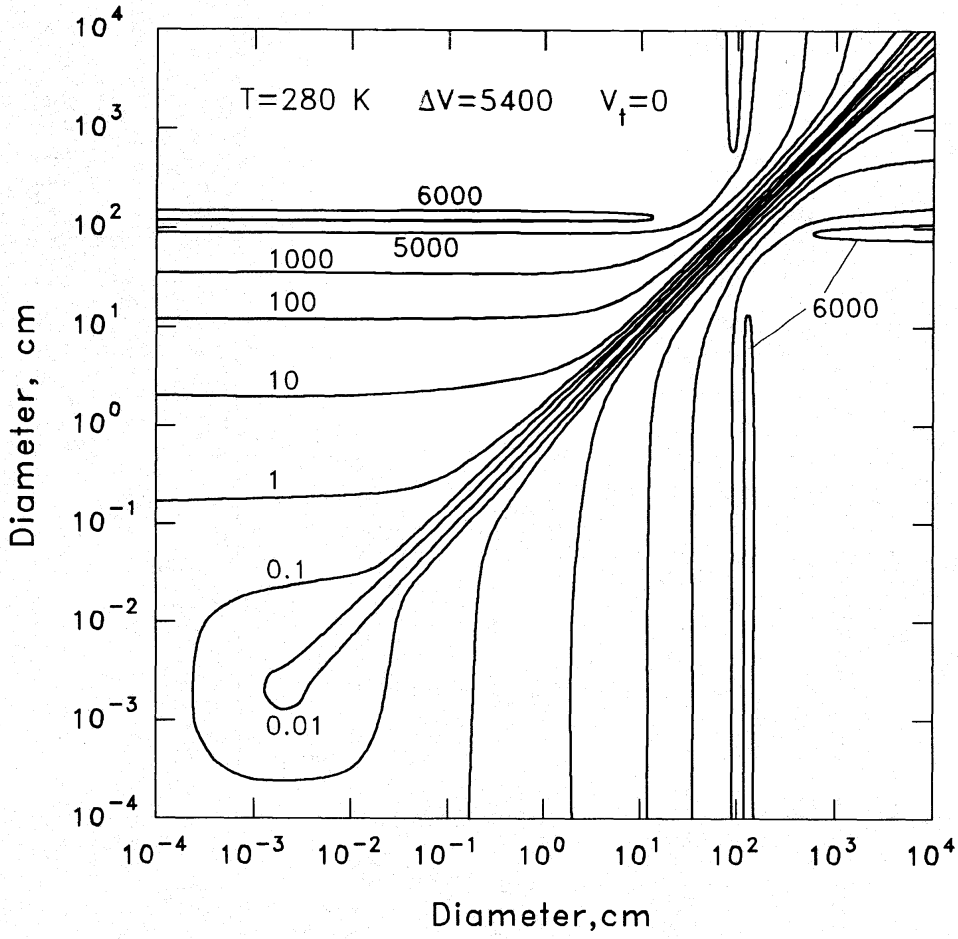

Figure 3. Relative velocities between two particles of unit density vs size in a laminar nebula. The nebular parameters are those of the model of Hayashi et al. (1985) at $r = 1$ AU, $z = 0$: $\rho = 1.4\times10^{-9}$ g cm^{-3}, $T = 280$ K, $\Delta V = 5400$ cm s^{-1}. Relative motions are due to thermal motion and radial and transverse velocities induced by non-Keplerian rotation of the gas. Thermal motion dominates for $d \lesssim 0.01$ cm; relative velocities are low for equal-sized bodies.

particle size are shown in Figs. 3 and 4 for one set of nebular parameters, with the gas assumed to be either laminar or turbulent.

IV. COUPLED MOTIONS IN A PARTICLE-GAS LAYER

Goldreich and Ward (1973) recognized that if a particle layer reached a density greater than that of the gas, the particles would dominate. Their velocities relative to the gas would not be given by Eqs. (13–15); rather, the particle layer would tend toward Keplerian motion, and the gas within that layer would be dragged with it. Weidenschilling (1980) showed by dimensional arguments that such shear would be unstable, and should produce turbulence in the particle layer. Any density gradient in the z direction is too small to prevent the dust layer from becoming turbulent. This localized shear-

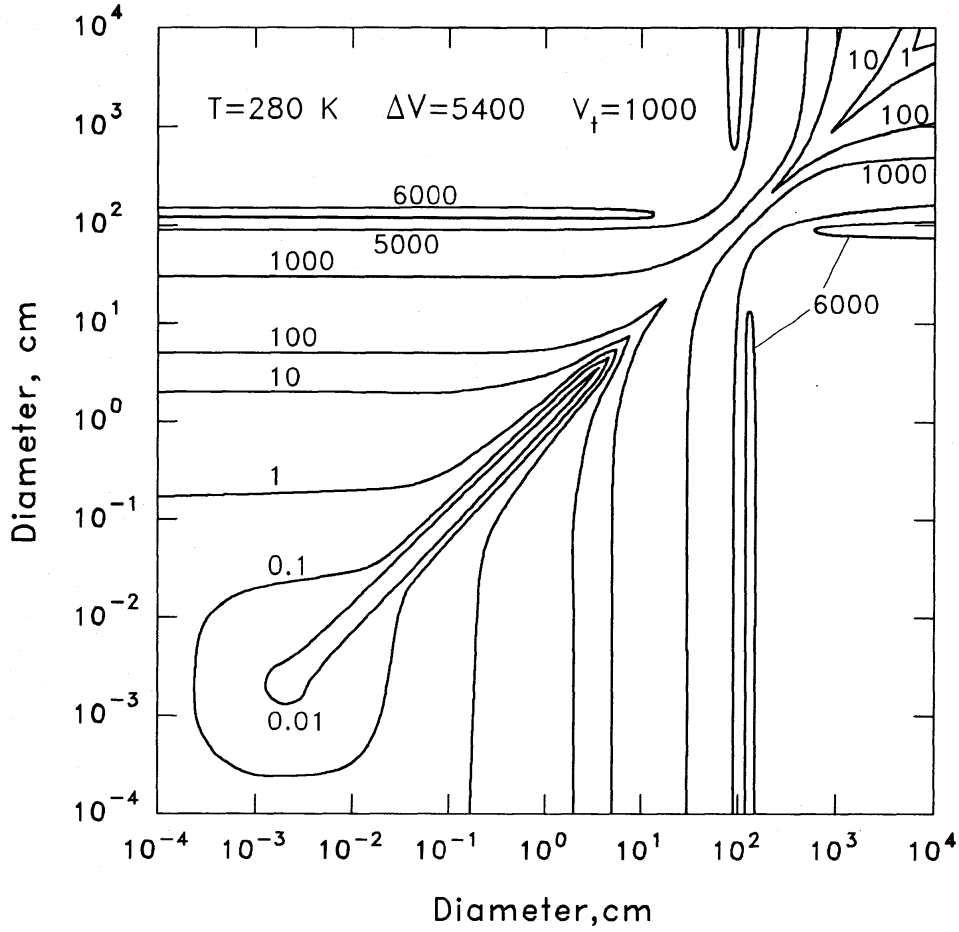

Figure 4. Same as Fig. 3, but with turbulence added; V_t = 1000 cm s^{-1}. Bodies with $d \simeq 100$ cm have $t_e \simeq 1/\Omega$; in this size range relative velocities are $\simeq V_t$ even for equal-sized bodies.

induced turbulence would occur even if the gaseous disk had no other source of turbulence, such as convection.

Nakagawa et al. (1986) developed an analytic solution for the coupled equations of motion for a two-phase inviscid system of particles and gas. The solutions are expressed as functions of the mass loading, i.e., the ratio of densities of the particle layer and the gas. To a good approximation, if the particles are small, the deviation from Keplerian motion within the layer is given by

$$\Delta V' = \Delta V/(1 + \rho_p/\rho) \tag{17}$$

where ρ_p and ρ are the space densities of the particles and gas, respectively. Nakagawa et al. assumed purely laminar motions; their solution is inappropriate if such a layer became turbulent. The presence of sufficiently large ($\gtrsim$1 cm) particles could cause some damping of turbulence, but it is not clear whether it is possible to have particles that are simultaneously large enough and abundant enough to damp the turbulence effectively. This question is

clearly a fruitful subject for future work.

The shear due to collective motion of the particle/gas layer becomes significant for mass loadings of order unity. Weidenschilling (1988*b*) speculated that this effect could lead to a quasi-stable, long-lived state. Formation of a layer with solids/gas mass ratio of order unity might induce enough turbulence to prevent further settling. Any decrease (increase) in layer's thickness would increase (decrease) the intensity of shear and turbulence, tending to restore its original state. It appears that the only escape from such a state would be a change in the particles themselves, i.e., coagulation into bodies large enough to decouple from the gas and settle in spite of the turbulence. This scenario needs to be tested by numerical modeling; preliminary results of such an effort are described in Sec. VI.B.

A. Viscosity in the Boundary Layer

The particle layer interacts with the surrounding gas primarily in a region of limited thickness, or boundary layer, in which the shear velocity and particle concentration vary most strongly. In a boundary layer of thickness δ surrounding the particle layer, the orbital velocity of the nebular gas changes by an amount ΔV. Shear flows with velocity scale ΔV and length scale δ develop turbulence when their Reynolds number $Re = \Delta V \delta / \nu$ exceeds a critical value $Re^* \sim 50$ to 500. The difference in orbital velocity is typically tens of meters per second and $\delta \sim 10^3$ km. For these values, the boundary layer is indeed turbulent. Thereafter the turbulent viscosity in the boundary layer becomes

$$\nu_t \sim (\Delta V \delta / Re^*). \tag{18}$$

In a system rotating at angular velocity Ω, the boundary layer thickness itself depends on the viscosity as

$$\delta \sim (\nu_t / \Omega)^{\frac{1}{2}} \tag{19}$$

leading to a crude mixing length estimate of the boundary layer viscosity:

$$\nu_t \sim \Delta V^2 / \Omega Re^{*2}. \tag{20}$$

For eddies with length scale δ, this implies turbulent velocities of order $\Delta V / Re^*$ in the boundary layer.

Shear flow has been studied in laboratories for decades, and the thickness of the boundary layer and the properties of the turbulence have been well characterized. In fact, numerical techniques now exist for modeling the structure of individual eddies and coherent structures within the turbulence. Canuto and Battaglia (1988) have derived expressions for turbulent viscosity and particle velocities that take into account anisotropic turbulence in a rotating system. However, for the purposes of modeling the nebula, homogeneous, isotropic turbulence in the shear-generated boundary layer is not a bad assumption. Several parameterizations exist for obtaining its magnitude. Champney and

Cuzzi (1990) have used two such parameterizations to study the turbulence induced by the particle layer in an otherwise laminar nebula. A simple model due to Prandtl, which is still an improvement over Eq. (20), is

$$\nu_t = C\delta^2(\nabla \times \mathbf{V}_g) \tag{21}$$

where $C \sim 0.1$ is a constant determined in the laboratory and $\mathbf{V}_g$ is the (vector) gas velocity. In more sophisticated models in computational fluid dynamics, a "two-equation" model is often used, in which the turbulence at a point is a balance between ongoing creation and dissipation processes, and is transported as is any other quantity. This latter model may be adapted to a two-phase environment in which the particles can damp turbulence, as well as generate it by maintaining the velocity gradient. Champney and Cuzzi (1990) have made preliminary studies of the merits of these two models, and further work is underway. The overall conclusion, at present, is that in the boundary layer $\nu_t \sim 10^{10}$ cm^2 s^{-1}. The turbulent viscosity calculated in this way for the boundary layer alone is much less than the values $\sim 10^{13}$ to 10^{15} cm^2 s^{-1} for turbulence through the entire thickness of the disk with $\alpha \sim 10^{-4}$ to 10^{-2}. The viscosity is confined to a boundary layer surrounding the particle layer, with thickness rather well estimated by Eq. (19).

Given the viscosity in the boundary layer, one may calculate the shear torque between the particle layer as a whole and the surrounding, more slowly rotating pressure-supported nebular gas. Goldreich and Ward (1973) assumed the particle layer acted as a rigid, impermeable rotating disk embedded within the gas. This situation, the Ekman problem, has been thoroughly studied in theoretical and laboratory work, and inspection of the analytical solutions leads to considerable insight into the more complex nebula problem (see, e.g., Batchelor 1967). The shear torque exerted between the disk and the fluid is

$$S = \rho \nu_t \Delta V / \delta = \rho \Delta V^2 / Re^*. \tag{22}$$

The result of this torque is a loss of angular momentum by the particle layer, which causes it to drift inwards at a rate that depends on the boundary layer's turbulent viscosity ν_t. Goldreich and Ward considered the orbital decay of a dust layer due to shear between it and the more slowly moving gas on either side. They did not discuss the effects on the gas, possibly thinking of it as merely providing a vast reservoir of angular momentum and not significantly affected by the particle layer. Nevertheless, interesting dynamical structure is present in both the particles and the gas in this important region of interaction, driven primarily by the turbulence that the particle layer itself generates. For example, the angular momentum lost by the particle layer is transferred to the gas in the boundary layer, which must then move outward (Weidenschilling 1980). Study of these motions in more detail requires a numerical model. Such a model is described in Sec. VI.B.

V. COAGULATION AND SETTLING OF PARTICLES

For an assumed structure of the nebular disk, the expressions in Sec. III yield the velocities of particles as functions of their sizes and location. In principle, one can use these values to compute the evolution of their spatial distribution in the disk. Also, by assuming mechanical properties (i.e., whether particles stick together in collisions), the evolution of the size distribution from some assumed initial state can be computed. Of course, the spatial and size distributions are coupled, and their evolution must be calculated simultaneously. In practice, all such efforts are subject to simplifying assumptions to render the problem tractable for analytic or numerical solution.

A. Coagulation in a Laminar Nebula

Safronov (1972) derived the settling velocity of a particle (Eq. 14). Because $V_z \propto z$, the distance from the central plane decreases exponentially with an e-folding time of $(\Omega^2 t_e)^{-1}$. If there is no turbulence and the particles do not coagulate, the entire dust layer becomes thinner and denser uniformly, in homologous fashion. Safronov considered settling with coagulation, in which a single large particle falls through a field of small grains and grows by sweeping them up. If only vertical motion of the particle is considered, it can grow to a maximum size $d_{\max} = \sigma_s/4\rho_s$, where σ_s is the surface density of the grain component of the disk. Plausible values of σ_s and ρ_s give $d_{\max}$ of the order of a few cm. The initial growth rate of the particle is exponential with a time constant $\lesssim 4\rho c/\sigma_s\Omega^2$. It reaches $d_{\max}$ (and $z \to 0$) in a few thousand orbital periods. Goldreich and Ward (1973) independently derived a similar result. These analytic models refer only to the first (and largest) particles to "rain out" to the central plane of the disk. Modeling the subsequent buildup of a particle layer and depletion of the smaller particles at large values of z requires numerical simulation. Nakagawa et al. (1986) described the settling and coagulation in a model that included collective effects of the particles upon the gas; i.e., ΔV varied with particle concentration. In order to make this problem analytically tractable, they had to make two mutually inconsistent assumptions: that growth was by the sweeping up of the small particles by the largest ones, and that settling was uniform, as if all particles had the same size.

Numerical models were developed independently by Weidenschilling (1980) and Nakagawa et al. (1981). These were one-dimensional models that computed the vertical distribution of particles at a given radius in the disk. The evolution of the size distribution due to coagulation was calculated in a series of levels, with mass transported between layers by settling (both assumed a laminar nebula, with transport only toward the central plane). Their results were very similar; assuming perfect sticking, a dense particle layer forms in the central plane within a few times 10^3 yr at $r = 1$ AU. The largest bodies grow to 10^2 to 10^3 cm in size, much larger than Safronov's value of $d_{\max}$, because the radial motion of the particles allows more growth. A modest

(but still significant) fraction of the mass of solids remains as small particles suspended in the gas to much later times (10^4–10^5 yr), due to their slow settling velocities. Thus, the disk could remain optically thick long after planetesimals formed. Both Weidenschilling and Nakagawa et al. assumed that settling of the large aggregate bodies would eventually result in gravitational instability of the particle layer, but neither model had fine enough spatial resolution to show this result directly. Also, they neglected the possibility of turbulence in the disk.

B. Turbulent Coagulation

Although it is widely accepted that the solar nebula passed through a stage as a turbulent accretion disk, there has been relatively little study of the consequences of turbulence for planetesimal formation. Most cosmogonical scenarios assume that planetesimals either formed despite turbulence (even values of α as large as 1/3), or else that any turbulence eventually decayed completely, and they formed after the disk became perfectly laminar. Particle coagulation in a turbulent disk has been considered by Wieneke and Clayton (1983), Morfill (1983,1988), Mizuno et al. (1988) and Mizuno (1989). These studies concerned radial transport of solid matter in the disk, while averaging the distribution and properties of particles vertically through the thickness of the disk. Only Mizuno computed actual size distributions of particles, rather than some effective mean size. The formation of planetesimals, whether by gravitational instability of a particle layer or direct collisional growth, appears to be intimately linked with concentration of particles toward the central plane of the disk. Thus, averaging through the disk thickness can cast little light on planetesimal formation.

Weidenschilling (1984) modeled the vertical distribution of particles at a given radius in a turbulent disk. The numerical method was based on the one-dimensional model described above (Weidenschilling 1980), but particles were allowed to settle toward the central plane only if they were large enough so that their settling velocities exceeded their turbulent diffusion velocities. The nebular model used had high turbulent velocities ($\alpha \sim 1/3$), as suggested by the convective disk models of Lin and Bodenheimer (1982). The vigorous turbulence resulted in high collision rates, and if perfect sticking was assumed, large particles would accrete much more rapidly than for a laminar disk. However, this assumption of perfect sticking seems unrealistic. If the particles were assigned plausible impact strengths, in the range 10^4 to 10^6 erg cm^{-3}, accretion came to a halt after a few centuries, with the largest aggregates (<1 cm in size), being destroyed in collisions as rapidly as they formed. Battaglia (1987) performed a similar calculation for the low-α disk model of Cabot et al. (1987*a*, *b*). He concluded that even for the lower turbulent velocities in that model nebula, unrealistically high strengths were required to allow aggregates to grow large enough to decouple from the gas and settle to the central plane.

The results of Weidenschilling and Battaglia can be readily understood

in terms of their assumptions about the collisional behavior of the particles. They assumed that for a given material there exists a critical energy density E_c, such that the target is shattered if an impact yields a higher value. For lesser impact energies, "cratering" erosion excavates and removes some amount of mass that is proportional to the impact energy; the excavated mass is then C_{ex} times the impact energy, where C_{ex} is the excavation coefficient. Then the excavated mass exceeds the projectile mass, i.e., there is net erosion, if the impact velocity V_i, is $>(2/C_{ex})^{\frac{1}{2}}$, and net mass gain occurs at lower V_i. E_c and C_{ex} are related by the condition that there is a largest cratering impact that the target can sustain without shattering. If the largest crater contains a fraction f of the target's mass, then $C_{ex} = f\rho_s/E_c$; typically, $f \simeq 0.1$ (Weidenschilling 1984).

Solid particles embedded in turbulent gas have relative velocities that increase with size, up to a maximum value roughly equal to the eddy velocity V_t for bodies with $t_e \simeq t_o$. It is significant that a body of this size has velocity of $\simeq V_t$ relative to *all* smaller bodies, up to those of its own size. This means that the target body will be eroded by collisions with smaller particles, losing mass rather than gaining, if V_t is $\gtrsim (2/C_{ex})^{\frac{1}{2}} = (2\,E_c/f\rho_s)^{\frac{1}{2}}$, or unless E_c exceeds the critical value $f\rho_s V_t^2/2$. If E_c is smaller than this value, solid bodies can never grow large enough to decouple from the turbulence ($t_e > t_o$). If E_c is $\gtrsim \rho_s V_t^2/2$, even collisions of equal-sized bodies will not disrupt them. For $f\rho_s V_t^2/2 < E_c < \rho_s V_t^2/2$, a body will grow due to impacts of much smaller bodies, but may be shattered by large impacts; its fate will depend on the size distribution of those it encounters. Taking $\rho_s = 2$ g cm^{-3}, $f = 0.1$, we see that, e.g., $V_t = 10^3$ cm s^{-1} requires $E_c \gtrsim 10^5$ erg cm^{-3} for collisional growth to occur. This simple model explains why Weidenschilling (1984) and Battaglia (1987) required high values of E_c in order to form large bodies by collisional coagulation. For any value of E_c we can find the maximum value of turbulent velocity that allows coagulation (although lower values of V_t do not necessarily assure it, unless the particles also stick when they collide).

Similar results can be obtained for the systematic velocities due to non-Keplerian rotation of the disk. However, bodies of comparable size (or t_e) have low relative velocities. The maximum relative velocity between bodies of very different sizes is $\simeq \Delta V$, so collisions always result in mass gain if $E_c \gtrsim f\rho_s \Delta V^2/2$. For typical values of ΔV ($\sim 10^4$ cm s^{-1} at 1 AU), growth is assured if $E_c \gtrsim 10^7$ erg cm^{-3}. This value is quite high, of the order of values measured for solid rock (Fujiwara et al. 1989). However, the model of impact behavior was extrapolated from experiments involving solid projectiles and targets; even for these, there is some indication that impact strength does not correlate with more conventional properties such as compressive strength (Fujiwara et al. 1989). It is possible that C_{ex} is much smaller than assumed by Weidenschilling, or even zero, i.e., that fluffy aggregates stick rather than "crater" each other below some critical velocity or energy density, as in the model of Donn (1990), discussed below.

C. The Problem of Particle Sticking

The major unsolved problem is the degree to which particles stick together in collisions, and the mechanism (or mechanisms) by which they adhere. It is common experience under a wide range of laboratory condition that very small ($\lesssim \mu$m-sized) particles stick together into larger aggregates. The dominant sticking mechanism in this size range is van der Waals bonding; this force is relatively insensitive to the compositions of the particles. Electrostatic forces may also play a role in coagulation. Weidenschilling (1980) argued that van der Waals forces alone would suffice to produce ~cm-sized aggregates of grains in a laminar nebula, where relative velocities are due to thermal motion and differential settling. This conclusion should be valid for a nebula with moderate turbulence ($\alpha \lesssim 10^{-2}$); particles in this size range are strongly coupled to the gas, so their turbulent motions are correlated and have little effect on their relative velocities.

The growth of larger bodies poses more of a problem. Relative velocities increase with size and differences in size (cf. Fig. 3), and there is a real possibility of outcomes other than sticking: rebound, erosion with net loss of mass, and even disruption of the colliding bodies. There are few relevant experimental data on the collisional behavior of weakly bonded aggregates. Weidenschilling (1988*c*) performed drop tests of unconsolidated pumice dust into a dust target and concluded that net mass loss would occur for impact velocities approximately $>10^3$ cm s^{-1}. Pinter et al. (1989) and Blum (1989) have conducted experimental collisions of sub-cm-sized fluffy aggregates at relative velocities up to a few meters per second. They found coagulation occurred with sticking probabilities of a few tens of percent. Their estimate that fragmentation would occur at relative velocities $\gtrsim$600 cm s^{-1} implies impact strengths of order 10^5 erg cm^{-3}. The aggregates consisted of glass spheres bonded by a coating of hydrocarbons; their degree of similarity to actual nebular material is uncertain.

Donn (1990) argues that collisions of porous bodies would result primarily in their interpenetration, with essentially complete agglomeration up to relative velocities of $\simeq 10^3$ cm s^{-1}, and net mass gain to $\simeq 5 \times 10^3$ cm s^{-1}. His analysis is based mainly on the behavior of porous materials under static compression, and needs to be verified by collisional experiments. Donn assumes very high porosities, making the aggregate bodies very compressible. We note that in most solar nebula models, peak velocities relative to most other particles are reached for roughly meter-sized bodies. Thus, bodies of this size are likely to be fairly well compacted, and may not coagulate as effectively as Donn's model implies.

As seen in Figs. 3 and 4, relative velocities decrease for bodies with sizes larger than ~10^2 cm, so if meter-sized bodies can form by collisional coagulation, then there is no obstacle to the formation of km-sized planetesimals. The crucial gap is in the centimeter-to-meter range. The collisional strengths that seem necessary for growth in this size (or velocity) range are higher than

expected for aggregates composed of small grains. There are alternatives to assuming that the aggregates are extremely strong. The relative velocities are caused mainly by differential motion due to non-Keplerian rotation of the gas. The maximum velocities are $\simeq \Delta V$, so there is less of a problem in the outer part of the disk where velocities are lower (Eq. 8). It is possible that the nebula's temperature and radial structure were such that ΔV was lower than implied by most nebular models. Less plausibly, accretion might have produced a narrow size distribution so that relative velocities of particles comprising most of the mass were less than ΔV. The most probable explanation is that a concentration of small (cm-sized?) aggregates decreased ΔV in a layer near the central plane (Eq. 17, cf. Sec. VI.B), allowing growth to proceed with lower relative velocities and minimizing collisional breakup.

VI. RECENT RESULTS OF NUMERICAL MODELS

The formation of planetesimals involves complex feedbacks between all of the processes described above, and no current model describes the full situation. Recent work has approached the problem from complementary perspectives, by emphasizing or suppressing different aspects of the problem. Below, we describe two such efforts which together paint a fairly realistic picture of, at least, the scope of possible situations. As a natural outgrowth of the discussion above, we first describe a model of particle growth by coagulation, which neglects coupling of the mean flow regimes and treats the gas eddy velocity in an *ad hoc* fashion. We then describe a complementary model of the fully coupled gas-particle flow dynamics near the midplane, which neglects particle growth and treats only a single typical particle size. The results of the two approaches are instructive and illustrate the variety of possible states in which a protoplanetary nebula might be found (possibly all, at different times). In the coagulation models, it is seen that (depending on the assumed turbulent gas velocity) a flattened state in which the particle mass density significantly exceeds that of the gas may or may not occur. In the coupled flow models, it is seen that even in a globally laminar nebula, relatively flat (thousands to tens of thousands of km vertical thickness) particle layers of mass density which exceeds that of the gas by 1 or even 2 orders of magnitude are stable against gravitational settling for particles smaller than tens of meters or so, due to shear-induced turbulence.

A. Coagulation and Settling with Turbulence

Weidenschilling has recently developed an improved code for modeling coagulation and settling in a turbulent disk. As in the earlier models (Weidenschilling 1980,1984) this is a one-dimensional computation, with the nebula divided into a series of layers at a given radial distance. The size distribution of particles in each layer is computed as it evolves due to collisions; sources of relative velocity include thermal motion, systematic settling, and turbulence.

In contrast to the earlier models, transport between layers by turbulent diffusion is computed explicitly. Particles can diffuse upward if their turbulent diffusion velocity (cf. Eq. 16) exceeds the settling velocity (Eq. 14). The spatial resolution (number and thickness of layers) is improved over earlier work, as is the resolution of the size distribution. A complete description of the model and results is published elsewhere (Weidenschilling 1993).

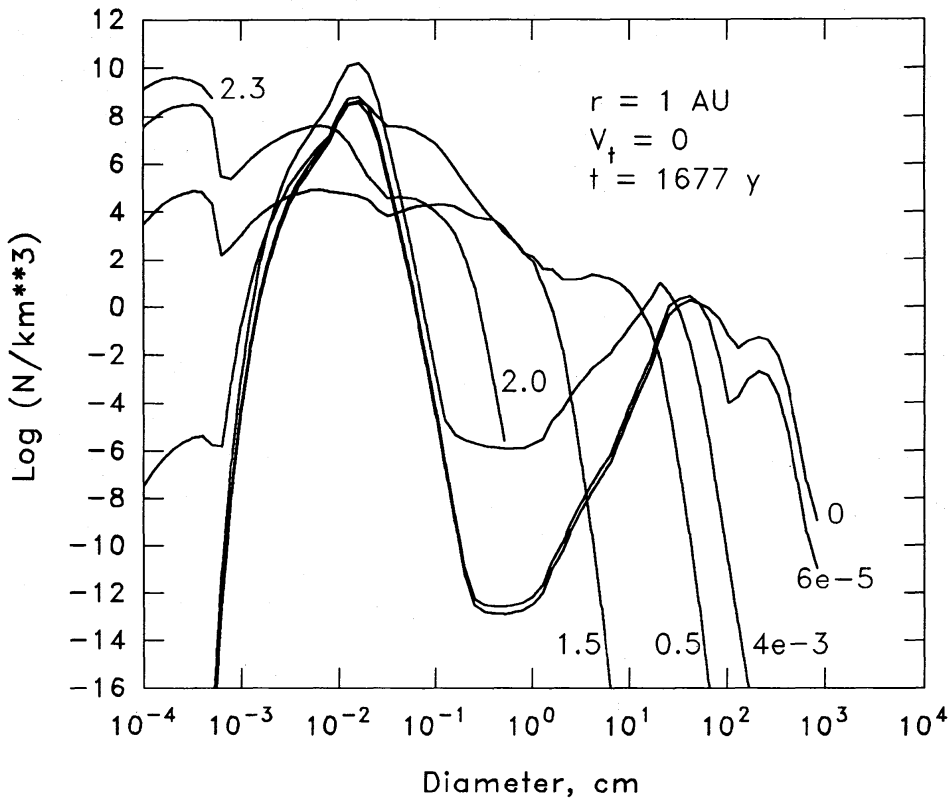

Figure 5. Size distribution at different levels for a laminar nebula, at $r = 1$ AU, at the time when the solids/gas mass ratio reaches unity at $z = 0$. Numbers give values of z in units of scale height H. At the highest level, aggregates reach a maximum size $\simeq 10^{-3}$ cm; the low density (4×10^{-3} times that at $z = 0$) allows rapid settling of larger particles. At $z = 0$, most of the mass is in bodies $\sim 10^2$ to 10^3 cm in size.

Because of uncertainties in the mechanisms for producing turbulence and its consequent strength, calculations are performed for "generic" turbulence. The largest eddies are assumed to have an arbitrary velocity V_t and size H, with a Kolmogorov spectrum of smaller eddies down to the appropriate inner scale (Eqs. 9 and 10). In the examples shown here, aggregate particles are assumed to have fractal properties with dimension 2.11 (Meakin and Donn 1988; Weidenschilling et al. 1989) in the size range 10^{-4} to 10^{-2} cm. At sizes >1 cm, their density begins to increase again to a limiting value of 1 g cm^{-3} at sizes $>10^2$ cm. The qualitative justification for this variation is that while grain assemblages formed by low-velocity collisions will be fluffy, higher-

velocity collisions of larger aggregates will cause compaction (the qualitative results are not affected by these assumptions about particle density).

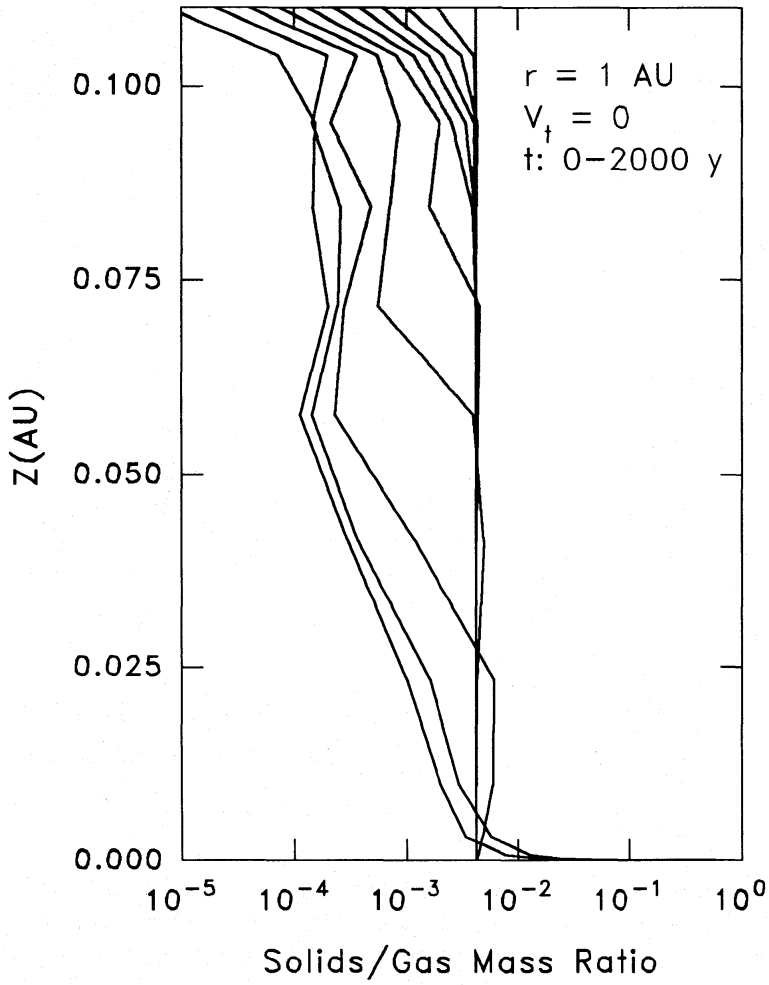

Figure 6. Vertical distribution of solids/gas mass ratio with time. At $t = 0$, the ratio is assumed to be 4.2×10^{-3}, independent of z. Contour interval is 200 yr.

In these calculations and those in Sec. VI.B, the nebular parameters are taken from the model of Hayashi et al. (1985). In the two examples shown here, an initial population of single grains, all of size 10^{-4} cm, is initially uniformly mixed with the gas. Perfect sticking is assumed in order to set a lower limit on the evolution time. The calculations are carried out until the particle/gas mass ratio reaches unity at $z = 0$, at which time collective effects become important, and a different method must be used (Sec. VI.B).

Figures 5, 6 and 7 illustrate the results for a purely laminar, nonturbulent disk. Figure 5 shows the size distribution at the various levels when the solids/gas ratio reaches unity, after a model time of 1677 yr (the much longer settling time reported by Weidenschilling et al. [1989] appears to be an artifact of the coarse resolution of their size distribution). Several peaks in the

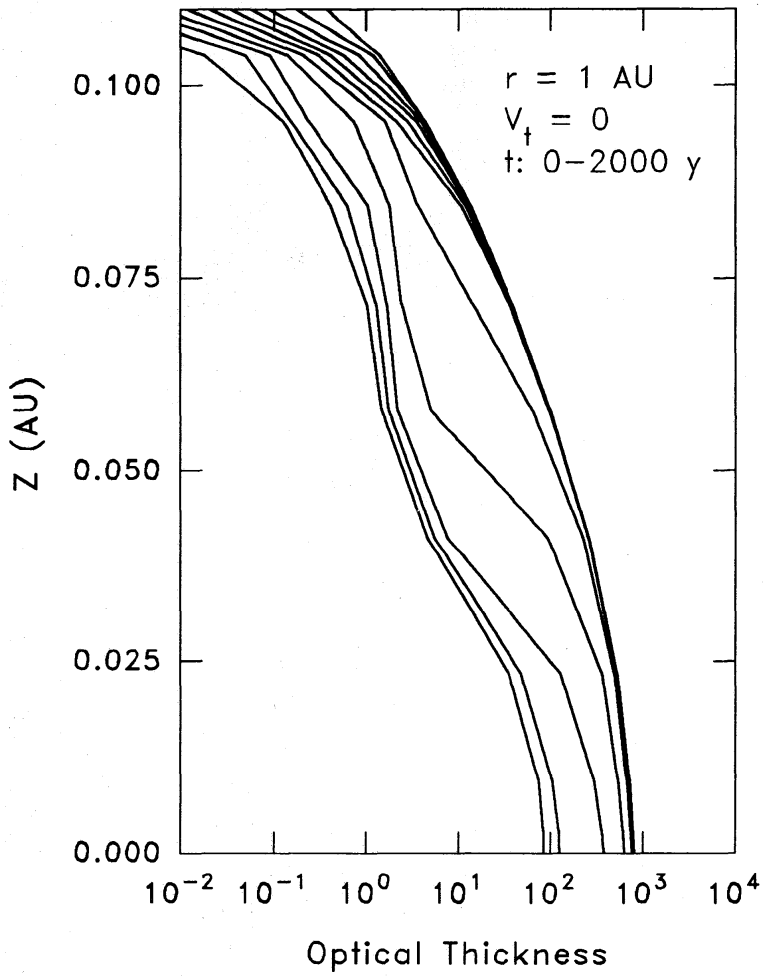

Figure 7. Cumulative distribution of normal optical thickness above a given value of z, vs time. Rosseland mean opacities from Pollack et al. (1985) are used. Opacities due to particles smaller than the peak emission wavelength are assumed proportional to the mass loading, with geometric extinction by (opaque) particles of larger size. The optical half-thickness drops from the initial value of $\simeq$800 to $\simeq$100 after 2000 yr, for perfect sticking of particles.

distribution correspond to sizes at which thermal motion (10^{-4} to 10^{-3} cm), vertical settling ($\sim 10^{-2}$ to 10^{-1} cm), and radial motion ($\sim$10 cm) dominate the collision rate. A fourth peak at 10^2 to 10^3 cm, appears at $z = 0$, where the largest bodies have settled. The changing vertical distribution of the dust/gas ratio is shown in Fig. 6, through most of the disk; the solids are depleted by $\simeq$1 order of magnitude in this time. Figure 7 shows the distribution of the optical thickness.

Turbulence with velocity of 10^3 cm s^{-1} has very little effect on relative velocities and coagulation rates of small particles, because their motions are highly correlated. However, the vigorous vertical diffusion of small particles affects the overall rate of growth and settling. There is very little variation of the size distribution with z (Fig. 8). The time to reach a high mass concentration at the central plane is much longer than for the laminar

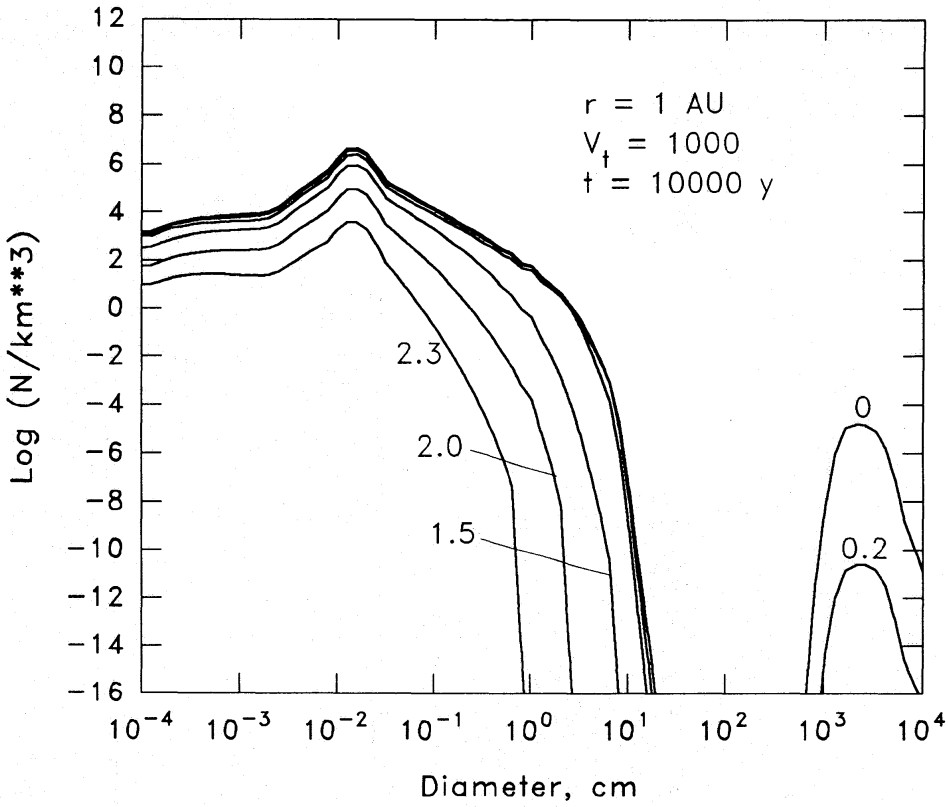

Figure 8. Same as Fig. 5, but for turbulence with velocity 10^3 cm s^{-1} through the thickness of the nebula. The size distribution has less variation with z, due to diffusion of particles between levels. Most of the mass is in large bodies $\sim 10^3$ to 10^4 cm near the central plane. The computation was halted after 10^4 yr, when solids/gas $\simeq 0.4$ at $z = 0$ (see text).

case, partly because particles must grow larger to settle appreciably, and also because the high-density layer near $z = 0$ is thicker due to stirring by the turbulence, and requires more total mass to reach a given solids/gas ratio. After $\gtrsim 10^4$ yr, most of the mass is in bodies $\sim 10^3$ to 10^4 cm in size. Bodies $\sim 10^2$ cm are strongly depleted because of the peak in radial velocity at that size, which causes them to grow rapidly through this size range, or to be swept up by the larger bodies.

From Fig. 9 it is seen that the dust/gas ratio varies only slightly with z through most of the disk's thickness, but it decreases steadily with time as small aggregates diffuse downward and are accreted by the large bodies near the central plane. (Figure 10 shows the evolution of the optical thickness.) The thickness of the densest layer is a few times 10^{-4} AU (5×10^4 km). The calculation was halted after 10^4 yr because the solids/gas mass ratio reached a peak value $\simeq 0.4$, and then began to *decrease*. This decrease is due to the fact that the settling rate for large bodies (actually, the rate of damping inclinations for Keplerian orbits by gas drag) is proportional to t_e^{-1} (Adachi et al. 1976), while the random velocity induced by turbulence (Eq. 16) varies as $t_e^{-1/2}$. Therefore, sufficiently large bodies ($t_e >> 1/\Omega$) are stirred more effectively

than they are damped. In this simulation, the solid bodies may continue to grow by collisions to much larger sizes, but will never form a layer that is sufficiently thin and dense to become gravitationally unstable.

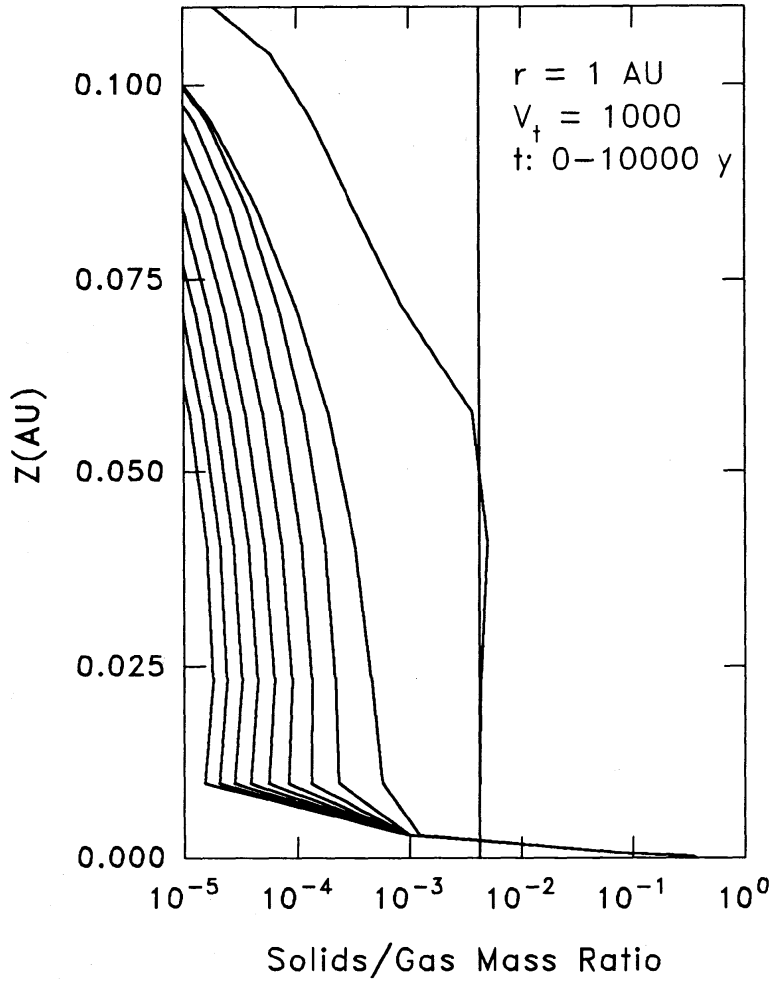

Figure 9. Vertical distribution of solids/gas mass ratio with time for $V_t = 10^3$ cm s^{-1}. Contour interval is 1000 yr.

These simulations assumed perfect sticking of particles and thus give only a lower limit to the time scales for growth and settling. If an arbitrary sticking efficiency β (≤ 1) is assumed, then the results are very similar, but with all time scales increased by a factor of $1/\beta$. The outcomes of such simulations may well be different if fragmentation is allowed, as the sticking efficiency would be expected to vary with relative velocity (or size). Also, the long time scale associated with the turbulent case implies that radial transport of solids would be significant. The small grains that are coupled to the gas will diffuse both inward and outward over a distance of order $(V_t H t)^{\frac{1}{2}}$, in this case more than 0.5 AU. In addition, orbital decay of the largest bodies exceeds 1 AU, meaning that they would be lost into the Sun (presumably replaced by others

spiraling inward from larger distances). Thus, the one-dimensional model is incomplete at best, and its results should be interpreted cautiously. Further progress will require a two-dimensional model with both vertical and radial resolution.

B. Fluid-Dynamical Modeling of a Dense Particle-Gas Layer

Simulations of settling with coagulation generally produce a significant concentration of large (meter-sized?) bodies toward the central plane of the disk. Whether the nebula is assumed to be laminar or turbulent, such a layer can attain a solids/gas mass ratio of order unity or greater. At such densities, coupling of the particles and gas, as described in Sec. III, becomes significant. The complex flow patterns that result must be modeled numerically by computational fluid dynamical methods. Current models are limited to a single particle size, without coagulation; in effect, particles interact with each other only by their mutual coupling with the gas (Champney and Cuzzi 1990; Cuzzi et al. 1993). The numerical methods used are described in the chapter Appendix.

This model is sufficiently stable and robust to allow modeling of particle layers with mass density exceeding that of the gas by more than 2 orders of magnitude. Due to the present neglect of particle collisional viscosity, these results are of questionable quantitative validity for particle mass densities much larger than that of the gas; nevertheless, major new qualitative aspects of the entire family of viscous, two-phase solutions may be readily observed in cases with a particle density of 1 to 10 times that of gas, where particle viscosity does not play a dominant role.

For example, Figs. 11 and 12 show the gas and particle velocities relative to their assumed unperturbed values (pressure supported orbital motion, $\Delta V = 5.4 \times 10^3$ cm s^{-1}, with zero radial and vertical velocity for the gas, Keplerian orbital motion with zero radial velocity and simple vertical settling for the particles). In this simulation, there is no turbulence in the disk, except that which is generated locally by shear near or within the particle layer. In both figures, initial and final particle density profiles are shown, with mass density along the top axis (the gas density at this location, chosen at 1 AU, is 1.4×10^{-9} g cm^{-3}). The fundamental property is the large vertical gradient in the gas orbital velocity; this leads to turbulence which diffuses the particles into a much thicker layer than that in which they were assumed to lie initially. In cases where a thicker initial layer was assumed, the layer flattens into the identical final state, which thus represents a steady-state balance between gravitational settling and vertical diffusion for these nebula and particle properties.

In model calculations to date, using the Schmidt number model describe in Sec. III (Cuzzi et al. 1993), it appears that particles of unit density must grow to at least 10^5 to 10^6 g (depending on location) before being able to settle out from the nebula into a gravitationally unstable state. If they are more "fractal" or fluffy than solid in nature, they need to become more massive by about

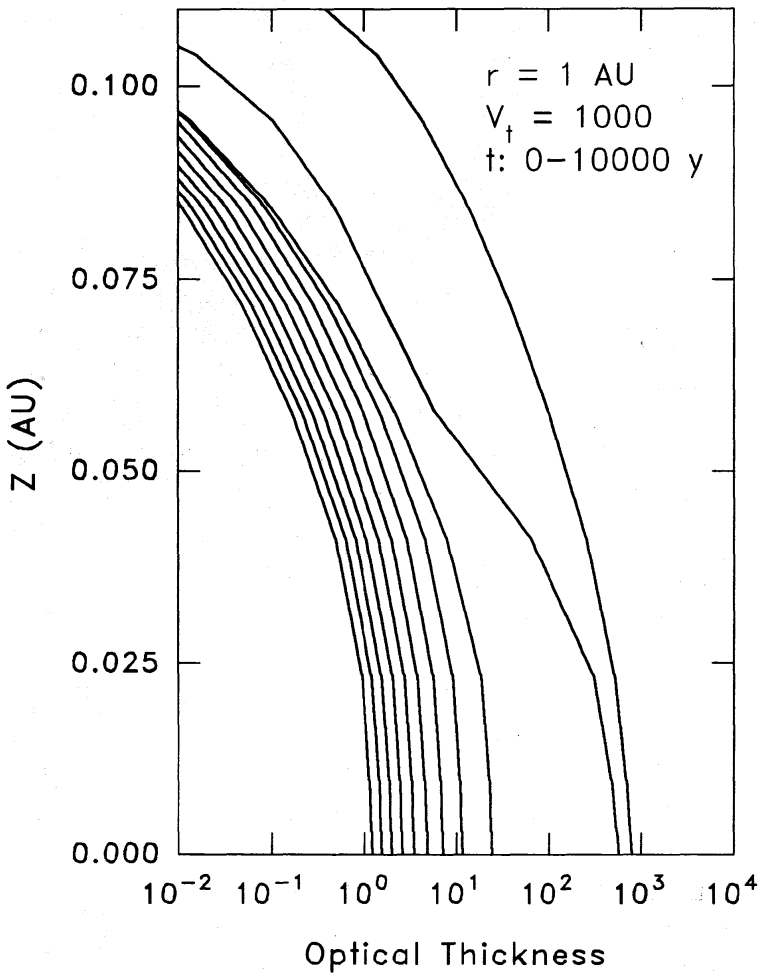

Figure 10. Same as 7, but with $V_t = 10^3$ cm s^{-1}. The nebula becomes optically thin at $r = 1$ AU on a time scale of 10^4 yr.

an order of magnitude. Initially flattened particle layers of mass density 10 to 100 times that of the gas are seen to "puff up" to vertical thicknesses of several thousand km, as long as particle diameters are $\lesssim$100 cm. For minimum mass solar nebulae, this keeps the particle layer mass density ρ_p well below the critical value for gravitational instability, confirming the conclusions of Weidenschilling (1980,1988) that collisional coagulation is a fundamental process in the formation of planetesimals.

The mean velocity profiles are seen to relate to the location of the particle layer. Well above the layer, when the particles exert no significant influence on the gas, the solutions of Weidenschilling (1977) and Nakagawa et al. (1986) are appropriate, i.e., particles experience a strong headwind in the pressure supported gas, their orbital velocity falls below Keplerian, and they drift radially inwards. At deeper levels within the layer, the particles are increasingly shielded from the headwind as the surrounding gas is speeded up more closely to the Keplerian velocity (several thousand cm s^{-1} faster

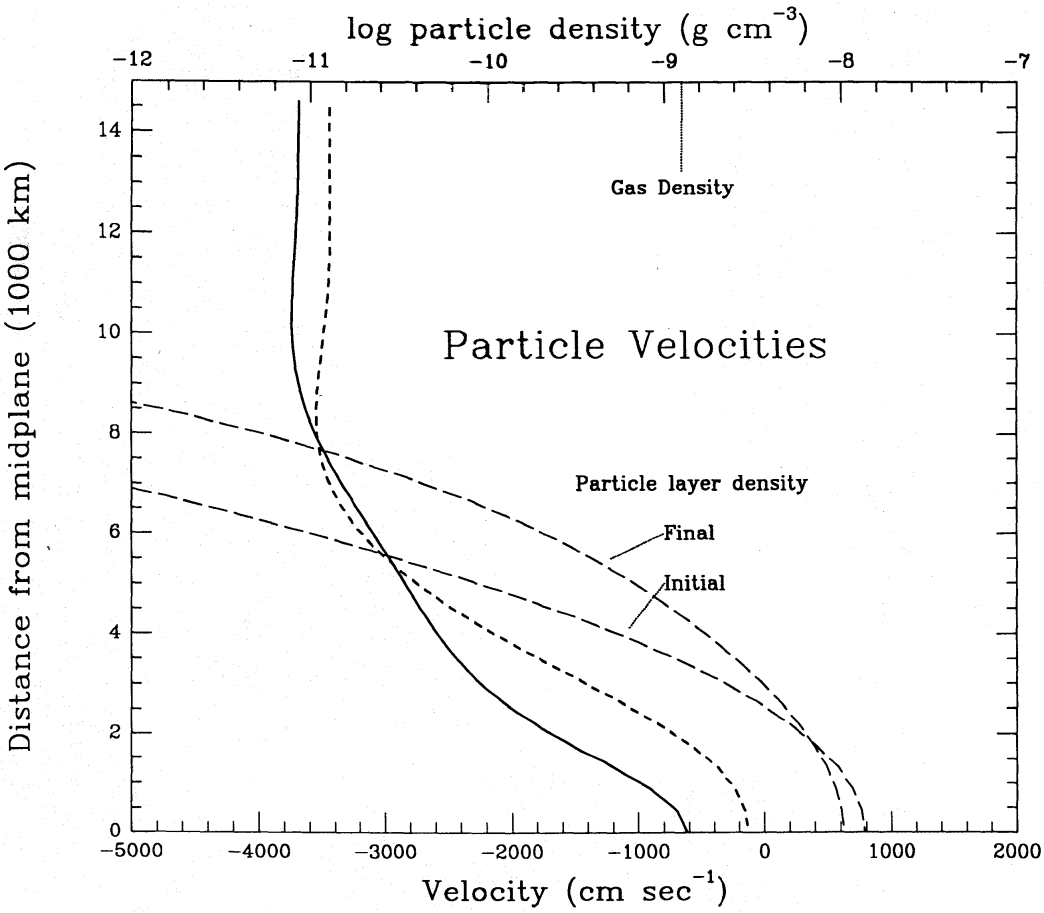

Figure 11. Particle velocities relative to planar Keplerian motion, for a layer of midplane mass density initially 10 times that of the gas at 1 AU. The particle orbital velocity profile is shown by the short-dashed curve, and the particle radial velocity profile is shown by the solid curve. The particles have d = 100 cm and ρ_s = 0.1 g cm^{-3}. The values shown are steady state, and have converged after ~100,000 Cray YMP timesteps, or ~2 yr. The initial and final profiles of mass density in the particle layer are shown by the long-dashed curves; the initial profile is flatter, and the layer "puffs up" over the course of the run due to the diffusive effects of shear-driven gas turbulence. The steady-state density of the center of the layer is ≃7 times the gas density, while the critical density for gravitational instability of the particle layer at this location is ~10^{-7} g cm^{-3}, or ~10 times larger.

than its pressure-supported value). The lack of a headwind causes the inward drift of the particles to diminish. Simultaneously, as the particles begin to drive the gas to orbital velocities which exceed its pressure-balanced value, the gas acquires an *outward* radial drift in the boundary layer consistent with Ekman layer analogy (Weidenschilling 1980). Another way to understand this is as the result of transfer of angular momentum between the more rapidly rotating particle layer and the more slowly rotating surrounding gas. The effect is confined to a region of thickness comparable to the boundary layer, because that is where the velocity gradients are sufficiently large to generate a significant viscosity and shear stress. The particle drift rates in the upper

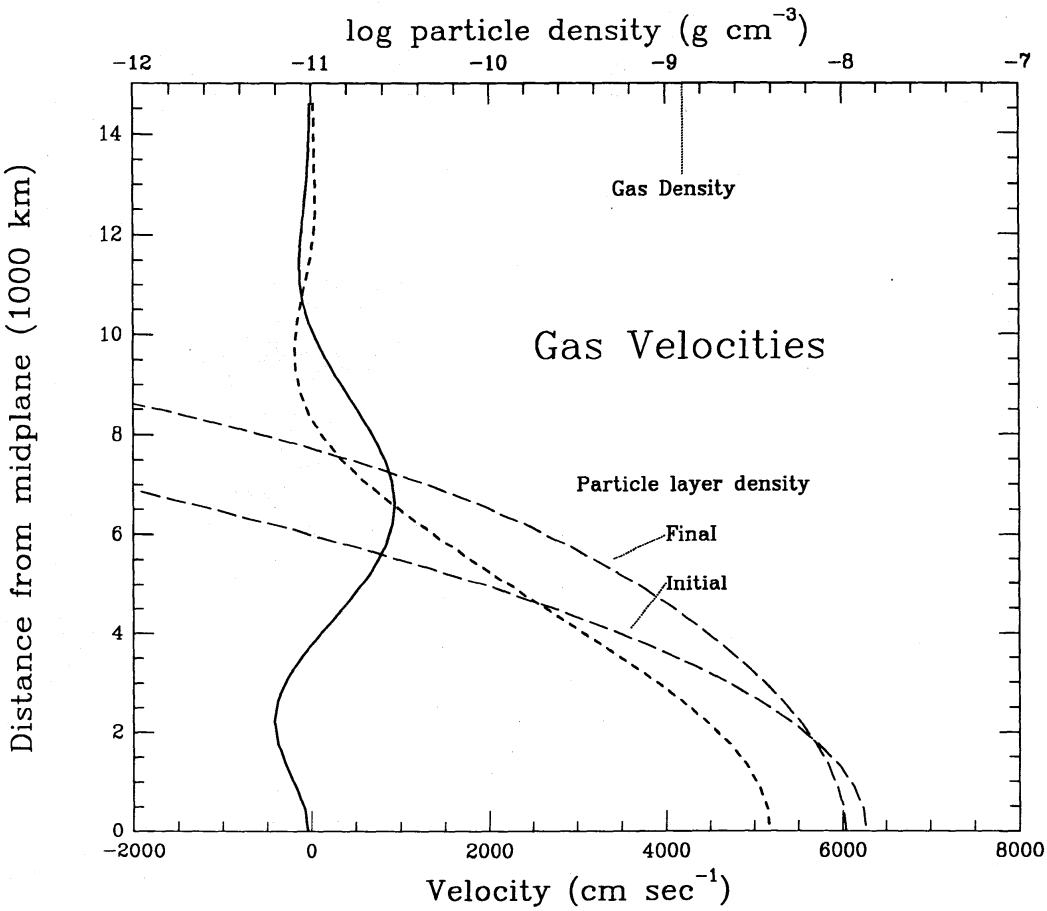

Figure 12. Gas velocities relative to pressure supported motion, for the final profile of mass density in the particle layer. The gas orbital velocity profile is shown by the short-dashed curve, and the gas radial velocity profile is shown by the solid curve. These are mean flow velocities; in addition, there is turbulence with fluctuations of comparable magnitude within the layer.

reaches of the layer are in fairly good agreement with the "Ekman" estimates discussed earlier, but deeper within the layer the solid material is less affected. Naturally, this assumes there is no source of turbulence other than the local shear, and that the gas viscosity at this stage and in this region is considerably less than the "alpha model" values of 10^{13} to 10^{15} cm^2 s^{-1}. Within the particle layer, the gas drifts inward along with the p rticles. In some cases, the vertical shear in the *radial* velocities can compete with the vertical shear in the *orbital* velocities in contributing to the viscosity, which emphasizes that this is a highly coupled problem.

In detail, the drift rates of gas and particles will probably change once viscosity due to particle collisions is included. For example, one simple estimate of the particle viscosity may be obtained from the expression widely used in studies of planetary rings (Goldreich and Tremaine 1978), using the expressions relating $\bar{v}_p^2$ to $\bar{v}^2$ from Eq. (16) (Dobrovolskis 1991, personal

communication);

$$\nu_p \sim \frac{v_p^2}{2\Omega}\left[\frac{\tau_o}{1+\tau_o^2}\right] \sim \frac{\nu_t}{2Sc}\left[\frac{\tau_o}{1+\tau_o^2}\right] \tag{23}$$

where τ_o is the dynamical optical depth of the layer (i.e., that due to particles of sizes comparable to the mean mass). Substituting, we obtain

$$\tau_o \sim \frac{\sigma_s}{\rho_s d} \sim \frac{\rho_p h}{\rho_s d} \sim 10^{-1} \tag{24}$$

where $\rho_p \sim 10^{-8}$ g cm^{-3} is the volume mass density in the particle layer, $d \sim 60$ to 100 cm is the typical particle diameter, and $\rho_s \sim 1$ g cm^{-3} is the density of an individual particle. The particle viscosity is comparable to the gas viscosity for the models presented above. When included, this effect will probably increase the inward radial drift of the densest part of the layer, causing a simultaneous increase in the outward flow of the surrounding gas.

VII. CONCLUSIONS

The preceding sections sketch out parts of the possible course of growth of particles from μm to km sizes in the context of current ideas about the solar nebula. It seems likely that planetesimal formation involved at least an early stage of collisional sticking and coagulation of particles. This process depended on poorly constrained properties of the nebula (e.g., temperature, pressure gradients, turbulence) and of the particles themselves (stickiness, mechanical strength, fractal dimension). Many variables need to be examined in more detail, especially collisional behavior of particle aggregates, for which relevant experimental data are sorely lacking.

It is apparent that if grains have a reasonable probability of sticking in collisions, then their size distribution and the vertical distribution of solids in the disk evolve rapidly compared with the expected astrophysical lifetime of the disk ($\sim 10^6$ yr). The assumption used by some observers, that size distribution is similar to that of interstellar grains, is not likely to be valid. Moreover, the actual size distribution may not resemble a simple power law, and may vary with location (radial and vertical) in the disk.

In the later stages of accumulation, collective effects (a dense particle layer dragging the gas) could have important consequences. Within the particle layer, ΔV is decreased, which may promote accretion of fragile aggregates; however, there is increased turbulence generated by the shear associated with this layer's motion, which can have the opposite effect. Complex flow patterns can occur, with radial gas motion inward at the central plane, and outward in the boundary layer. In addition to vertical sorting (larger bodies nearer the center of the layer), there may be radial segregation as well, if smaller particles are entrained in the boundary layer. If this stage

is long-lived, there could be significant mixing of solids formed at different distances from the Sun. It is not clear that any such effects would leave visible traces in the meteoritic record, but the possibility should be considered. The computational fluid dynamical model described here is still in the early stages of development; the obvious next step will be to include a spectrum of particle sizes and coagulation within the particle layer.

The later stage ($\sim$ m to km) of planetesimal formation has not yet been examined in detail. Two (at least) possible outcomes can be inferred. If the bodies in the turbulent, shearing layer near the central plane can grow large enough by mutual collisions, they may decouple from the gas sufficiently to allow further settling. In that case, there might be gravitational instability in a layer of > meter-sized bodies, rather than one made of dust grains. On the other hand, a plausible amount of global turbulence, e.g., due to convection in the disk, could prevent gravitational instability no matter how large the solid bodies grow. In that case, collisional coagulation will be the only mechanism of growth at all sizes. These outcomes are model dependent; indeed, both could have occurred in different parts of the disk, or at different times.

Regardless of the actual mechanism by which planetesimals formed, that process was not so efficient as to deplete the dust in the solar nebula and render the disk optically thin. Detection of dust in a circumstellar disk does not rule out the presence of planetesimals, or even planets, within it.

The parts of this chapter do not make a seamless and self-consistent scenario for the origin of planetesimals. One should remember that the accretion of planets from planetesimals involves growth in size by a factor 10^4, while the formation of km-sized bodies from μm-sized grains covers 9 orders of magnitude. There is still room for plenty of work within that range.

APPENDIX: MODELING OF A PARTICLE-GAS LAYER

Here we present for reference a self-consistent formulation for computational fluid dynamical simulation of a viscous two-phase (particles plus gas) layer near the central plane of the solar nebula. A more detailed description of this model is given by Champney and Cuzzi (1990) and Cuzzi et al. (1993).

A. Solution of the Mass and Momentum Equations

The full equations of motion in cylindrical coordinates are:

$$\frac{\partial \rho}{\partial t} + w\frac{\partial \rho}{\partial z} + \rho\frac{\partial w}{\partial z} + u\frac{\partial \rho}{\partial r} + \frac{\rho \partial u}{\partial r} + \frac{\rho u}{r} = 0 \qquad \text{(A.1)}$$

$$\frac{\partial w}{\partial t} + w\frac{\partial w}{\partial z} + \mathrm{v}\frac{\partial w}{\partial r} + \frac{1}{\rho}\frac{\partial P}{\partial z} =$$

$$-\frac{GM}{R^3}z - A\rho_p(w - w_p) + \frac{1}{\rho}\frac{\partial \tau_{zz}}{\partial z} + \frac{1}{\rho r}\frac{\partial (r\tau_{zr})}{\partial r} \qquad \text{(A.2)}$$

$$\frac{\partial u}{\partial t} + w\frac{\partial u}{\partial z} + u\frac{\partial u}{\partial r} + \frac{1}{\rho}\frac{\partial \rho}{\partial r} =$$

$$\frac{\mathrm{v}^2}{r} - \frac{GM}{R^3}r - A\rho_p(u - u_p) + \frac{1}{\rho}\frac{\partial \tau_{zr}}{\partial z} + \frac{1}{\rho r}\frac{\partial (r\tau_{rr})}{\partial r} - \frac{\tau_{\theta\theta}}{\rho r} \qquad \text{(A.3)}$$

$$\frac{\partial \mathrm{v}}{\partial t} + w\frac{\partial \mathrm{v}}{\partial z} + u\frac{\partial \mathrm{v}}{\partial r} =$$

$$\frac{-u\mathrm{v}}{r} - A\rho_p(\mathrm{v} - \mathrm{v}_p) + \frac{1}{\rho}\frac{\partial \tau_{z\theta}}{\partial z} + \frac{1}{\rho r}\frac{\partial (r\tau_{r\theta})}{\partial r} + \frac{\tau_{r\theta}}{\rho r} \qquad \text{(A.4)}$$

$$\frac{\partial \rho_p}{\partial t} + w_p\frac{\partial \rho_p}{\partial z} + \rho_p\frac{\partial w_p}{\partial z} + u_p\frac{\partial \rho_p}{\partial r} + \rho_p\frac{\partial u_p}{\partial r} + \frac{\rho_p u_p}{r} =$$

$$\frac{\partial}{\partial z}\left[\frac{\nu_t}{Sc}\frac{\partial \rho_p}{\partial z}\right] + \frac{\partial}{\partial r}\left[\frac{\nu_t}{Sc}\frac{\partial \rho_p}{\partial r}\right] \qquad \text{(A.5)}$$

$$\frac{\partial w_p}{\partial t} + w_p\frac{\partial w_p}{\partial z} + u_p\frac{\partial w_p}{\partial r} = \frac{-GM}{R^3}z - A\rho(w_p - w) \qquad \text{(A.6)}$$

$$\frac{\partial u_p}{\partial t} + w_p\frac{\partial u_p}{\partial z} + u_p\frac{\partial u_p}{\partial r} = \frac{\mathrm{v}_p^2}{r} - \frac{GM}{R^3}r - A\rho(u_p - u) \qquad \text{(A.7)}$$

$$\frac{\partial \mathrm{v}_p}{\partial t} + w_p\frac{\partial \mathrm{v}_p}{\partial z} + u_p\frac{\partial \mathrm{v}_p}{\partial r} = -\frac{u_p\mathrm{v}_p}{r} - A\rho(\mathrm{v}_p - \mathrm{v}) \qquad \text{(A.8)}$$

where u, v, w are the mean velocity components in the radial (r), transverse (θ), and vertical z directions, and ρ is the spatial density. Quantities without subscripts refer to the gas, and the subscript p refers to the particles. A is a drag coefficient (equal to $1/\rho t_e$), $R^2 = r^2 + z^2$, ν_t is the turbulent kinematic viscosity of the gas phase, and Sc is a dimensionless parameter known as the Schmidt number, which is discussed in Sec. III. The terms τ_{ij} are the components of the viscous stress tensor for the gas phase. In the above equations, no similar terms are included for particle viscosity. Initially in the nebula, the particle volume density is sufficiently low that this is an acceptable approximation. However, as increasingly dense layers are studied, this does become a concern.

Champney and Cuzzi (1990) and Cuzzi et al. (1993) present a numerical model which includes all of the viscous and nonlinear terms, and overcomes the significant numerical challenges by using a perturbation technique in which an analytical solution is first subtracted from the problem. The analytical, or unperturbed, solution consists of Keplerian orbital motion for the particles, pressure supported orbital motion for the gas, and hydrostatic equilibrium in the vertical direction for the gas. In the unperturbed solution, the vertical particle velocity is merely the terminal settling velocity. These solutions are subtracted from the exact equations, and the remaining terms are solved numerically.

In Secs. III and IV we discussed solutions for the mean gas and particle velocities, and for the gas turbulent (eddy) viscosity. The effects of the turbulent boundary layer on dispersion of the particles is modeled as a diffusion term in the particle mass conservation equation (Eq. A.5) where the term ν_t/Sc is the particle diffusion coefficient D. Certain subtleties are associated with derivation of the diffusion term from averaged versions of the exact equations (see Champney and Cuzzi 1990), but models of this form are extensively used in two-phase fluid engineering applications.